New Approaches to the Identification of Sources and the Onset of Stealth Coronal Mass Ejections

Yu. S. Zagainova[a], * and V. G. Fainshtein[b]

[a]*Institute of Terrestrial Magnetism, Ionosphere and Radio Wave Propagation, Russian Academy of Sciences, Moscow, Russia*
[b]*Institute of Solar—Terrestrial Physics, Siberian Branch, Russian Academy of Sciences, Irkutsk, Russia*
*e-mail: yuliazagainova@mail.ru

Abstract—New approaches to the identification of sources and the onset of stealth coronal mass ejections (CMEs) are discussed based on the stealth CME of July 7, 2012. It is shown that the generation of this stealth CME is accompanied by various manifestations of short-term and small-scale activity in the region of its formation in the form of bursts of UV radiation (a microflare), as well as the activation and movement of loop-like structures. The features of the behavior of the photospheric magnetic field in the region of observation of the microflare are studied. The formation of a frontal CME structure there can be considered evidence that the stealth CME is generated in a solar atmospheric region with detected manifestations of solar activity.

1. INTRODUCTION

Most CMEs detected by coronographs are associated with various manifestations of solar activity in the lower corona (low coronal signatures—LCSs): flares, filament eruptions, EUV waves, dimming regions, jets, etc. It turns out that there are CMEs observed in the field of view of coronographs that, according to various sources, are generated on the visible surface of the Sun but are not accompanied by LCSs. It was long assumed that such CMEs form on the back of the Sun. Apparently, Robbrecht et al. (2009) were the first to show that CMEs accompanied by LCSs observed by the coronograph were generated on the visible side of the Sun. The properties of CMEs accompanied and unaccompanied by LCSs were compared (Ma et al., 2010). Howard and Harrison (2013) suggested that, if there is no LCSs accompanying a CME, it is most likely due to insufficient temporal and spatial resolution, as well as insufficient spectral sensitivity of the instruments. These CMEs are currently referred to as stealth CMEs.

D'Huys et al. (2014) examined the largest to date sample of stealth CMEs, a total of 40 events detected in 2012. The same authors also proposed a definition of stealth CMEs as coronal mass ejections that occur in the visible hemisphere of the Sun but are unaccompanied by LCSs. In addition, they showed that the studied stealth CMEs have on average a significantly lower speed (≈300 km/s) than CMEs accompanied by LCSs (≈435 km/s). Stealth CMEs turned out to be narrower (average angular size of ≈25°) than CMEs accompanied by LCSs (average angular size of ≈35°).

Finally, we note that the position angle (PA) of stealth CMEs are mainly observed near PA ~0° (or equivalently ~360°), although it can take any value within the range of 0° to 360°.

Alzate et al. (2017) detected the associated LCSs for many stealth CMEs using advanced methods to process solar images obtained in different spectral channels with instruments with high temporal and spatial resolution.

The same stealth CMEs analyzed by D'Huys et al. (2014) were analyzed in this work. The authors concluded that all 40 studied events are associated with LCSs (small solar flares, jets, or filament eruptions) in one form or another. Alzate et al. (2017) concluded that, overall, stealth CMEs are caused by observational limitations and limitations of image processing methods.

Nevertheless, the problem of identification of the sources of many stealth CMEs on the Sun remains. Therefore, the development of new approaches to identify the origin of stealth CMEs is an urgent problem. We assume that the generation of stealth CMEs should always be accompanied by some manifestations of solar activity, not only at the time of its formation but also after the start of the movement of the generated CME. This can be explained by the fact that the coronal matter and the magnetic field are disturbed in the CME region. Recording the consequences of such disturbances can serve as the key to finding the source of stealth CMEs.

Even a visual analysis of the processes of the generation of many CMEs accompanied by LCSs with UV images of the Sun makes it possible to conclude that
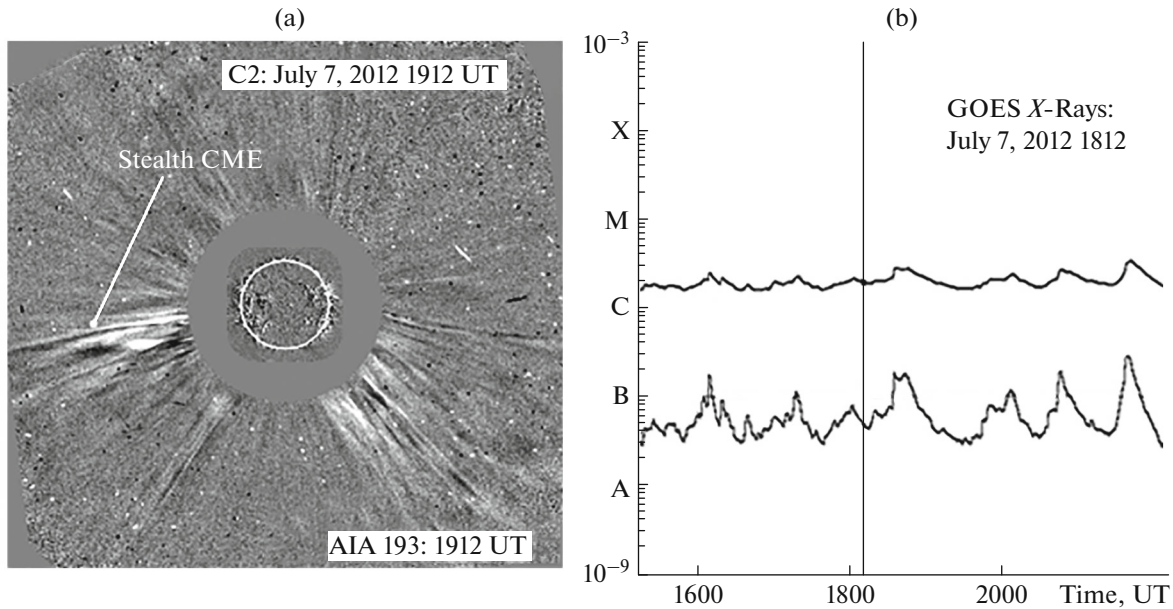
Fig. 1. (a) A differential image of the corona showing the stealth CME of July 7, 2012, in the FOV of the LASCO C2 coronograph, (b) the X-ray radiation intensity integrated over the solar disk according to GOES data (to illustrate that there is no X-ray flare associated with the "stealth" CME generation).

their formation can also be accompanied by various short-term and small-scale activities. We assumed that such short-term and small-scale solar activity can also accompany the emergence of stealth CMEs. One can also expect that this solar activity associated with the generation and movement of stealth CMEs will also manifest itself in variations of the photospheric magnetic field.

A study of the generation of CMEs accompanied by LCSs based on data with high temporal and spatial resolution revealed the formation of the frontal structure (FS) of mass ejections in the lower corona (e.g., Fainshtein and Egorov, 2015; Zagainova and Fainshtein, 2015; Grechnev et al., 2016). The problem of whether stealth CME FS generation can be detected remained open until recently. The stealth CME FS was discovered for the first time by the authors of this work for an event that occurred on June 16, 2010 (Zagainova et al., 2018). However, the search for the stealth CME FS remains an important area of research on the initiation of mass ejections unaccompanied by LCSs.

It was established that Forbush decreases can occur when stealth CMEs reach the Earth's orbit (Heber, et al., 2015). Some researchers (Kilpua et al., 2014; Nitta and Mulligan, 2017) linked the generation of noticeable geomagnetic disturbances with the impact of stealth CMEs on the Earth's magnetosphere. He et al. (2018) showed that even a weak CME without visible features in the lower corona produced a relatively intense geomagnetic storm. This became possible because this stealth CME was trapped between streams of fast and slow solar winds.

The goal of this study is to test new approaches proposed by the authors to identify stealth CME sources on the Sun based on the event detected on July 7, 2012, with the LASCO C2 coronograph.

2. DATA AND METHODS OF ANALYSIS

We studied the solar activity accompanying the onset of stealth CMEs detected in the field of view (FOV) of the LASCO C2 coronograph onboard the SOHO spacecraft on July 7, 2012 (1812:05 UT) (Fig. 1a). This CME was first identified as a stealth CME by D'Huys et al. (2014). They showed that this CME was generated on the visible hemisphere of the Sun. The fact that this CME was not accompanied by an X-ray flare (see Fig. 1b) or a flare in the optical range, as well the fact that there was no dimming, which often accompanies the onset of CMEs, confirms the assumption that this CME is a stealth CME. However, Alzate et al. (2017) identified the source of this stealth CME. They concluded that this event originated from the active region (AR) of NOAA 11520 and found that this CME was actually accompanied by LCSs such as flares and filament eruption. It was shown that the series of flares that began on July 6, 2012, and continued on July 7, 2012, preceded the generation of the discussed filament in the LASCO C2 FOV. Several sympathetic filament eruptions were observed in close connection with these flares (Alzate et al., 2017).

Here are the main characteristics of this CME from the catalog (https://cdaw.gsfc.nasa.gov/CME_list/): central PA = 101°, angular width = 24°, linear speed (V_{lin}) = 480 km/s, acceleration = 120 m/s², mass =

1.9×10^{14} g, and kinetic energy = 2.2×10^{29} erg. Note that the image quality of the analyzed CME in the LASCO C2 FOV is low, which is typical for many stealth CMEs. Note that this stealth CME was also detected by the COR2 coronograph, which is part of the Sun−Earth *Connection Coronal and Heliospheric Investigation* (SECCHI) toolkit (Howard et al., 2008) onboard the Solar-Terrestrial Relations Observatory spacecraft A, B (STEREO; Kaiser et al., 2008).

We believe that, while the LCSs manifestations established by Alzate et al. (2017) associated, in their opinion, with the generation of the analyzed CME (which was previously labeled a stealth CMEs) can be considered grounds to exclude this CME from the category of stealth CME, at the same time, they are not an unconditional basis for this. Note, for example, that there are "too many" manifestations of flare activity that accompanied the generation of the discussed CME discovered by Alzate et al. (2017). This does not make it possible to associate specific manifestations of this activity with the formation of the analyzed CME. The filament eruption, which the authors associate with CME generation, occurred near the active region in which CME was formed. The question of whether this eruption is really associated with CME formation remains open. In fact, we are still dealing with the CME unaccompanied by the LCSs manifestations typical of most CMEs. Recall that the integrated X-ray flux received by GOES does not make it possible to associate the studied event with any X-ray flare on the visible disk of the Sun or, therefore, to identify the exact location of the initiation of this CME. Thus, we will continue to arbitrarily call the analyzed CME as a stealth CME, putting the word *stealth* in quotation marks.

In this article, we try to identify the manifestations of solar activity associated with the generation of a stealth CME based on a new approach that we tested using the "stealth" CME detected on June 16, 2010 (Zagainova et al., 2018). We assume that the characteristic activity associated with the formation of the "stealth" CME is a short-term and small-scale activity in the form of radiation bursts in the EUV range in several channels and the activation (in some cases, eruption) of small, loop-shaped structures. The authors of this article believe that the detection of the generation of the stealth CME FS, inside which the region with the considered activity occurs, is convincing evidence of the close relationship of short-term and small-scale activity with CME emergence. Features can also manifest themselves in the dynamics of the photospheric magnetic field in the region of stealth CME formation.

The "stealth" CME generation was studied with multiwavelength data from the high temporal and spatial resolution instruments of the *Atmospheric Imaging Assembly* (AIA, Lemen et al., 2012) onboard the Solar Dynamics Observatory (SDO) (Pesnell et al., 2012).

The AIA provides multiple simultaneous, full-disk images of the corona and transition zone up to 0.5 Rs above the solar limb with a spatial resolution of 1.5 arcseconds and a 12-second time resolution. We used solar observations in several spectral channels (94 Å (temperature corresponding to the temperature response function peak, $T = 6.5 \times 10^6$ K), 304 Å ($T \approx 0.05 \times 10^6$ K), 171 Å ($T = 0.6 \times 10^6$ K), 193 Å ($T = 1.6 \times 10^6$ K), 211 Å ($T = 2 \times 10^6$ K), and 131 Å ($T = 10.1 \times 10^6$ K), (Lemen et al., 2012) (see also Fig. 4 in (Downs et al., 2012)) to identify the probable site of the formation of the "stealth" CME and to detect various manifestations of solar activity there. We used differential images of the Sun in different channels of the AIA instrument of the SDO spacecraft to determine the FS of the studied CME.

The magnetic field variations accompanying the generation of the "stealth" CME were studied based on field vector measurements of the *Helioseismic and Magnetic Imager* (HMI) (Schou et al., 2012) onboard the SDO. In this case, the measurements of the magnetic field were corrected with allowance for the π-ambiguity of the determination of the transverse component of the field with the method proposed by Rudenko and Anfinogentov (2014).

We divided the AR in which the "stealth" CME supposedly formed into circular segments (see Fig. 2a for examples of such segments) and selected the segment that turned out to be the source of the most intense short-term increase in radiation in several EUV channels (94, 131, 171, 193, 211, 304, 335 Å) (see Fig. 2a, red segment) to identify the solar activity associated with the formation of the considered CME.

Let us describe in detail the identification procedure in the studied AR for the required segment. A time dependence of the maximum radiation intensity in each of the above channels was constructed for each UV channel within each segment allocated on the solar disk. As a result, we found bursts of UV radiation intensity in four segments (these segments are highlighted by circles in Fig. 2a). The values of the UV radiation intensity in each channel was then normalized to the background radiation. To do this, a region of background radiation of the segment in which no jumps in radiation intensity were observed over the entire observation time interval was selected within each of the four segments, i.e., areas corresponding to the quiet Sun were identified. Then, the maximum value of the UV radiation intensity Ia was divided by the corresponding average value of the background radiation of the segment Iq at each time point in each of the four segments. As a result, the dependence of the maximum UV intensity on time In(t) = Ia(t)/Iq(t) normalized to the background radiation was obtained for each of the segments in each channel. It turned out that we identified the largest-in-amplitude UV-radiation burst, a UV microflare, in one of the four segments.
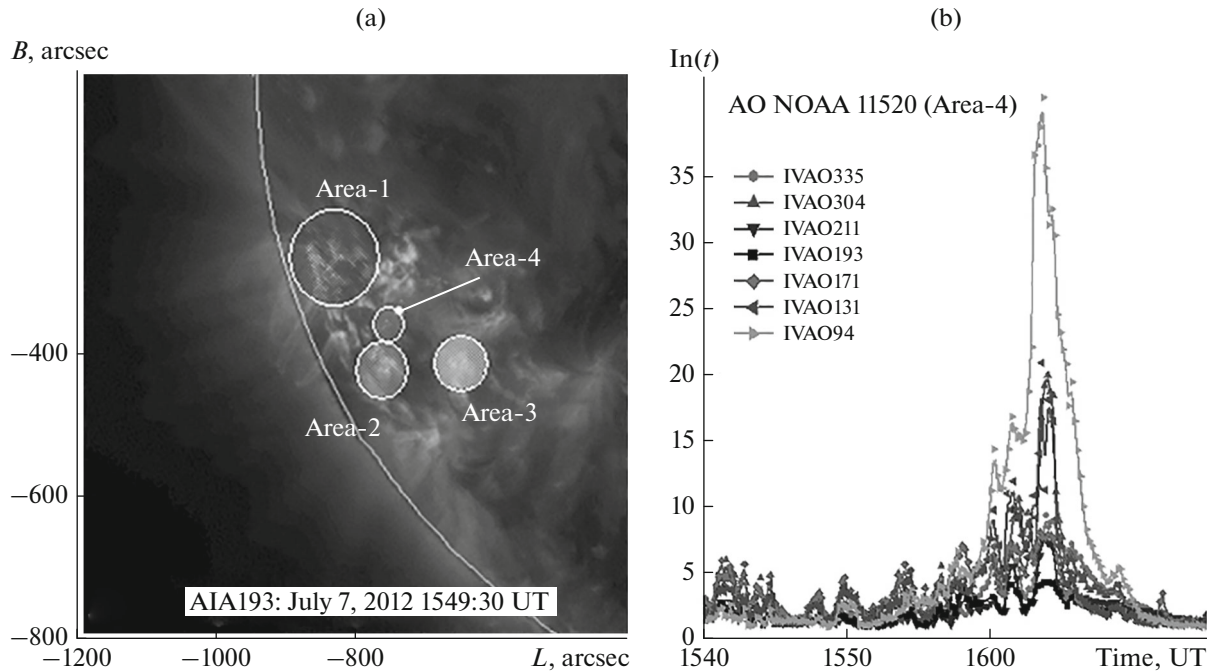
Fig. 2. Example of the method to identify segments in which small-scale solar activity was observed in the studied AR. It includes (a) the image in the SDO/AIA 193 Å channel with the selected segments Area-1, Area-2, Area-3, and Area-4, within which bursts of UV radiation were observed and (b) the time dependence of the maximum radiation intensity in different AIA channels in the Area-4 segment, in which a UV microflare of maximum intensity was observed (as compared to the other segments).

We assumed that the segment with the most intense UV radiation burst was the site of the generation of the studied "stealth" CME. This assumption is also supported by the fact that this segment and the studied "stealth" CME detected in the LASCO C2 FOV are in one quarter by Pas, NE. Thereafter, small-scale activity was analyzed only in this segment. The activation and eruption of several small-scale loop-like structures were detected at this site, in intense radiation bursts at the probable site of the "stealth" CME generation.

3. RESULTS

3.1. Solar Activity During "Stealth" CME Initiation

We tried to detect small-scale, rapidly changing activity in the solar atmosphere from the data on solar radiation in several UV channels for the studied event. We assumed that such activity could occur near the "stealth" CME generation site.

Figure 2b shows the time dependences $In(t) = Ia(t)/Iq(t)$, which are the ratios of the maximum radiation intensity within the studied segment Ia to the average intensity Iq in a quiet region in the same segment. These intensities were obtained in different spectral channels. The most powerful radiation was observed in the 94 Å channel, and the radiation with the weakest intensity was in the 193 Å channel. The

radiation sources on all channels were small areas on the solar disk (less than $20'' \times 20''$)

It also follows from Fig. 2b that the duration of radiation bursts is maximal for the burst with the highest intensity (radiation in the 94 Å channel) and minimal for the burst with the lowest intensity (radiation in the 193 Å channel). Note that the radiation turned out to be the most intense in the 131 Å channel and the least intense in the 211 Å channel for the previously studied event on June 16, 2010 (Zagainova et al., 2018). However, as in the 131 Å channel, in the 94 Å channel the temperature corresponding to the maximum radiation intensity Tm $\gg 10^6$ K was the characteristic temperature of the corona (Tm = 10.1×10^6 K in the 131 Å channel and Tm = 6.5×10^6 K in the 94 Å channel).

It is possible that the maximum radiation intensity can correspond to different sources in the sselected area in Fig. 2a at different points in time when a burst of UV radiation was observed in several channels. Figure 3, which presents the difference images of the solar section in the 193 Å channel, shows that the brightest source of radiation in this channel during the burst of UV radiation (from 1552 UT to 1612 UT) is the region in which a loop-like structure was observed, possibly a small-scale AR filament. This is confirmed by observations of the Sun in the 304 Å channel.

Several bright "intensity nodes" appeared in the northeastern area of the considered part of the Sun
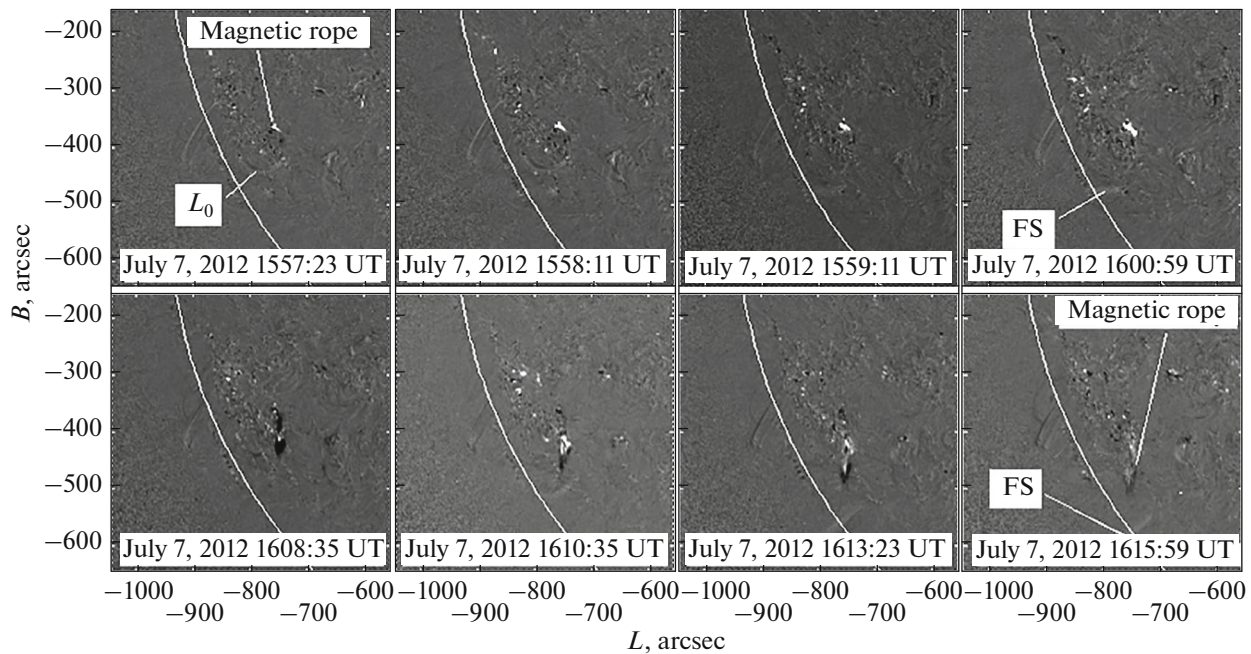
Fig. 3. Generation of the FS of the "stealth" CME of July 7, 2012, in AR NOAA 11520. The images obtained at different times in the AIA 193 Å channel show an eruptive magnetic rope (or a small-scale AR filament), as well as a loop-like structure L_0 and an element of the FS.

during this time period. These nodes also undoubtedly contribute to the resulting intensity of the radiation burst in the 94 Å channel. The increase in the radiation brightness in the region of the eruptive magnetic rope possibly reflects the manifestation of the standard model of a flare when the rising eruptive filament leaves rarefaction of the solar material (plasma) underneath itself, and the outer parts of the plasma and magnetic field with opposite polarity rush into this region, which, in the end, leads to magnetic reconnection and additional plasma heating at the apex of the resulting flare loop.

Another manifestation of the short-term and small-scale activity that accompanies the generation of the stealth CME is the already mentioned eruption of a magnetic rope (AR filament) and the activation of a loop-like structure (Fig. 3).

Filament eruption is currently believed to trigger most CMEs (Schmieder et al., 2013). The authors of this article note that more than 80% of filament eruptions result in CMEs. A number of studies observed the generation of the CME FS associated with filament eruption (or another type of magnetic rope) based on the SDO/AIA data. It was shown that the FS occurs due to the effect of a moving filament on the surrounding corona (Fainshtein and Egorov, 2015; Grechnev et al., 2016). Apparently, we were the first to detect the formation of the stealth CME FS based on the stealth CME detected on June 16, 2010 (Zagainova et al., 2018). It turned out that the FS generation was also detected for the "stealth" CME discussed in this arti-

cle. A moving FS formation was observed in the time interval 1559:11 UT–1615:59 UT in Fig. 3. In contrast to the stealth CME of June 16, 2010, the "stealth" CME FS generation in this case was preceded by the eruption of the magnetic rope. We can assume in this case that the detected eruption of the magnetic rope is also nothing more than an eruptive, small-scale AR
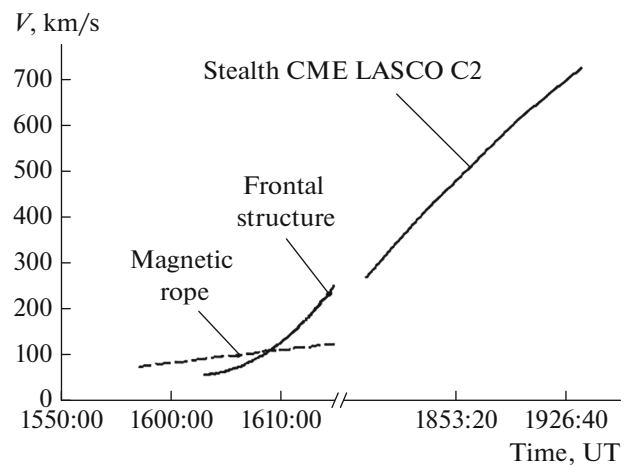
Fig. 4. Velocity profiles $V(t)$ of the eruptive magnetic rope (small-scale AR filament) and the "stealth" CME FS in the images of the Sun in the 193 Å channel and the "stealth" CME in the FOV of the LASCO C2 coronograph (where $V(t)$ is the projection velocity of the movement of the studied structures in the image plane).
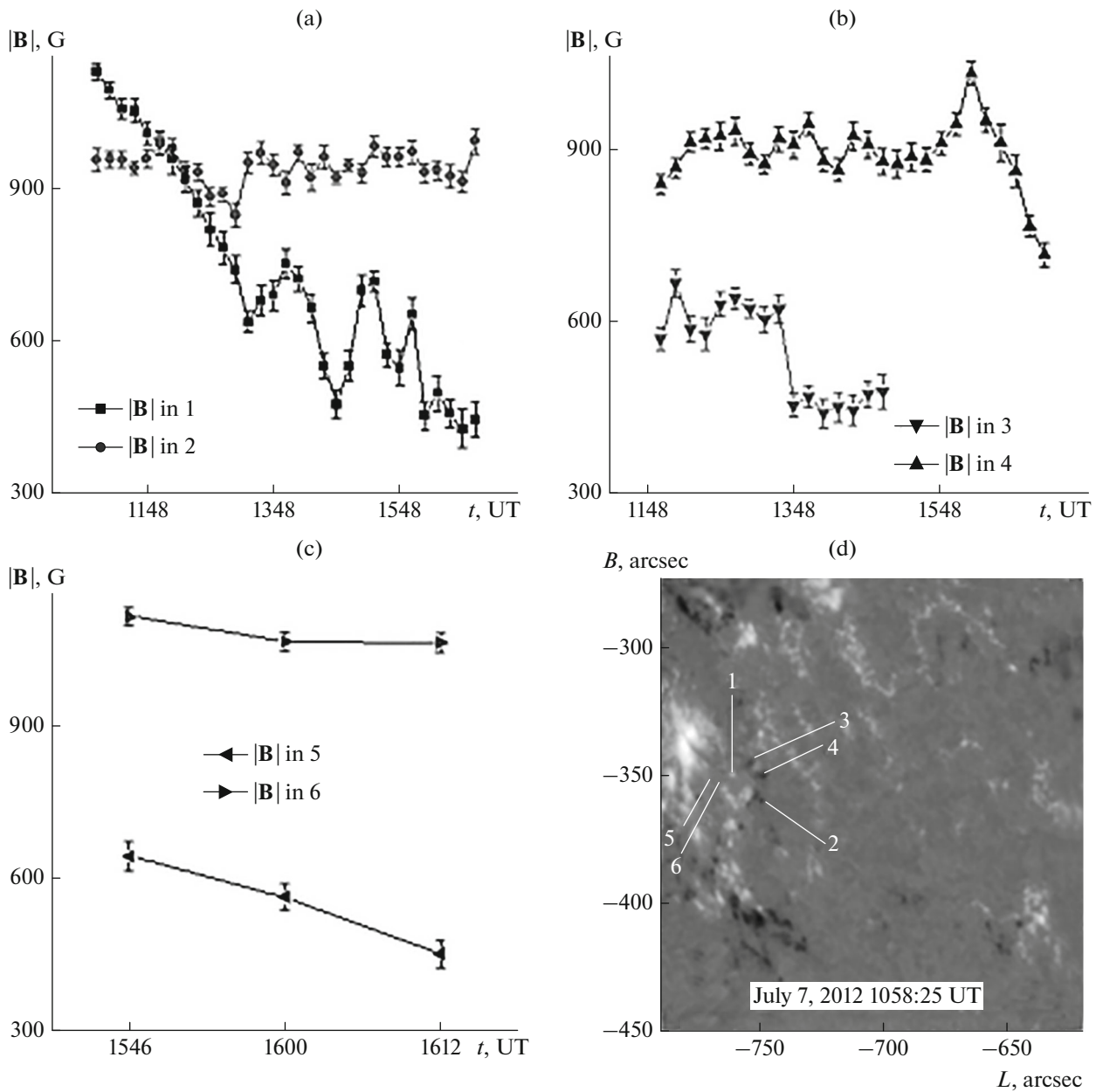
Fig. 5. Variations of values of |**B**| in the selected "magnetic nodes" in the region of generation (Area-4) of the "stealth" CME of July 7, 2012. Key: the magnetic nodes for which noticeable changes in the magnetic field were observed over the entire observation period from 1030 UT to 1630 UT are numbered 1–5 (see panel (d)).

filament that possibly served as a trigger for the generation of the studied "stealth" CME.

Our results differ from those obtained by Alzate et al. (2017). Alzate et al. (2017) suggested that the so-called "sympathetic" eruptions observed over a long period of time, from 1018 UT to 1618 UT, are responsible for the initiation of the CME on July 7, 2012. They failed to identify the eruption of the magnetic rope (AR filament), the activation of the loop-like structure, and the FS generation of the investigated "stealth" CME. It also turned out that the studied CME FS is generated in a shorter period of time (1559–1616 UT), when the starting time of the eruption of a small-scale magnetic rope is taken into account.

Figure 4 shows the CME FS velocity profiles obtained with the use of differential images of the Sun in the 193 Å channel and images of the corona in the FOV of LASCO C2 and C3, as well as velocities of the magnetic rope and FS. By comparing the behavior of FS and CME velocities in the LASCO FOV, We can conclude that this "stealth" CME is gradual and that its velocity monotonically increases with time. The

velocity of the magnetic rope is less than the FS velocity for some time, but then the FS begins to move faster.

As mentioned above, a separate CME type that occurs on the visible surface of the Sun is observed in the field of view of coronographs but is unaccompanied by LCSs is considered to be a stealth CME. This primarily implies that there are no manifestations of solar activity on a large spatial scale or powerful flares. It may turn out, based on our results and individual results of Alzate et al. (2017) and other authors, that stealth CMEs take relatively weak mass ejections, the generation of which is accompanied by different manifestations of small-scale solar activity in the lower corona.

3.2. Magnetic Field Variations at the Site of the "Stealth" CME Generation

The small scale of the selected Area-4 segment and the studied structures in it should be noted before the discussion of the results of the study of the behavior of the magnetic field in the "stealth" CME generation segment. As in the case of the stealth CME of June 16, 2010, the "stealth" CME of July 7, 2012, was also accompanied by variations in the photospheric magnetic field. However, the nature of such variations in detail turned out to be different from the features of the field changes in the event of June 16, 2010. In the considered event, before the start of the UV microflare, there was no noticeable or long-term decrease in the absolute values of the radial component of the field or the field magnitude of both signs. After its completion, there was no increase in these field characteristics, as was the case on June 16, 2010. The change in the photospheric magnetic field that was common to both events was the change in $|\mathbf{B}|$ in detected "magnetic nodes" with increased values of the magnetic field. It is possible that some of the small-scale structures of the magnetic field, which we arbitrarily called "magnetic nodes" due to their small spatial size, are associated with the generation/disappearance of pores in the studied AR. The magnitude $|\mathbf{B}|$ decreased in some "magnetic nodes" and slightly changed in others, either monotonously or against the background of oscillations for several hours, but the magnetic field did not increase. Figure 5 shows examples of the behavior of $|\mathbf{B}|$ over time in some "magnetic nodes" in the stealth CME generation region. The only change that can be noted is the disappearance of the "magnetic node 3" at ~1520 UT (Figs. 5b and 5d), where the highest values of UV radiation intensity were observed in the Area-4 segment. This is apparently due to the restructuring of the magnetic field configuration in the studied area before the onset of the microflare and the generation of the "stealth" CME.

4. CONCLUSIONS

The details of the generation of the "stealth" CME detected on July 7, 2012, were studied, and LCSs accompanying the formation of this CME was detected.

1. We found that the "stealth" CME detected on July 7, 2012, in the FOV of LASCO C2 and C3 was accompanied by various manifestations of short-term and small-scale activity at the site of the alleged generation of this CME. This activity included an increase in the radiation intensity in different EUV channels, the eruption of a magnetic rope (small-scale filament), and the activation of a loop-like structure.

2. The generation of the "stealth" CME FS was detected with solar observations in the AIA 193 Å channel.

3. Variations in the photospheric magnetic field were studied in the area of the "stealth" CME generation. It was found that there is an increase in the magnetic field $|\mathbf{B}|$ in the region in which the "stealth" CME is generated, in the so-called "magnetic nodes." $|\mathbf{B}|$ mainly decreases either monotonously or against the background of intense oscillations a few hours before and after the event.

4. The time profiles of the velocity of the eruptive magnetic rope (small-scale filament) and the "stealth" CME FS were studied. It was concluded from the analysis of the CME FS velocity profiles observed in the FOV of both SDO/AIA and LASCO C2 C3 that the studied stealth CME is "gradual," i.e., its speed monotonically increases with distance.

CONFLICT OF INTEREST

The authors declare that they have no conflict of interest.

REFERENCES

Alzate, N. and Morgan, H., Identification of low coronal sources of "stealth" coronal mass ejections using new image processing techniques, *Astrophys. J.*, 2017, vol. 840, no. 2, id 103.

D'Huys, E., Seation, D.B., Poedts, S., and Berghmans, D., Observational characteristics of coronal mass ejections without low-coronal signatures, *Astrophys. J.*, 2014, vol. 795, no. 1, id 49.

Downs, C., Roussev, I.I., van der Holst, B., et al., Understanding SDO/AIA observations of the 2010 June 13 EUV wave event: Direct insight from a global thermo-

dynamic MHD simulation, *Astrophys. J.*, 2012, vol. 750, no. 2, id 134.

Fainshtein, V.G. and Egorov, Ya.I., Initiation of CMEs associated with filament eruption, and the nature of CME related shocks, *Adv. Space Res.*, 2015, vol. 55, no. 3, pp. 798−807.

Grechnev, V.V., Uralov, A.M., Kochanov, A.A., et al., A tiny eruptive filament as a flux-rope progenitor and driver of a large-scale CME and wave, *Sol. Phys.*, 2016, vol. 291, no. 4, pp. 1173−1208.

He, W.Y., Liu, D., Hu, H., et al., A stealth CME bracketed between slow and fast wind producing unexpected geo-effectiveness, *Astrophys. J.*, 2018, vol. 860, no. 1, id 78.

Heber, B., Wallmann, C., Galsdorf, D., et al., Forbush decreases associated to stealth coronal mass ejections, *Cent. Eur. Astrophys. Bull.*, 2015, vol. 39, pp. 75−82.

Howard, T.A. and Harrison, R.A., Stealth coronal mass ejections: A perspective, *Sol. Phys.*, 2013, vol. 285, nos. 1−2, pp. 269−280.

Howard, R.A., Moses, J.D., Vourlidas, A., et al., Sun Earth Connection Coronal and Heliospheric Investigation (SECCHI), *Space Sci. Rev.*, 2008, vol. 136, nos. 1−4, pp. 67−115.

Kaiser, M.L., Kucera, T.A., Davila, J.M., et al., The STEREO mission: An introduction, *Space Sci. Rev.*, 2008, vol. 136, nos. 1−4, pp. 5−16.

Kilpua, E.K.J., Mierla, M., Zhukov, A.N., et al., Solar sources of interplanetary coronal mass ejections during the solar cycle 23/24 minimum, *Sol. Phys.*, 2014, vol. 289, no. 10, pp. 3773−3797.

Lemen, J.R., Title, A.M., Akin, D.J., et al., The Atmospheric Imaging Assembly (AIA) on the Solar Dynamics Observatory (SDO), *Sol. Phys.*, 2012, vol. 275, nos. 1−2, pp. 17−40.

Ma, S., Attrill, G.D.R., Golub, L., and Lin, J., Statistical study of coronal mass ejections with and without distinct low coronal signatures, *Astrophys. J.*, 2010, vol. 722, no. 1, pp. 289−301.

Nitta, N. and Mulligan, T., Earth-affecting coronal mass ejections without obvious low coronal signatures, *Sol. Phys.*, 2017, vol. 292, no. 9, id 125.

Pesnell, W.D., Thompson, B.J., and Chamberlin, P.C., The SOLAR DYNAMICS Observatory (SDO), *Sol. Phys.*, 2012, vol. 275, nos. 1−2, pp. 3−15.

Robbrecht, E., Patsourakos, S., and Vourlidas, A., No trace left behind: Stereo observation of a coronal mass ejection without low coronal signatures, *Astrophys. J.*, 2009, vol. 701, no. 1, pp. 283−291.

Schmieder, B., Démoulin, P., and Aulanier, G., Solar filament eruptions and their physical role in triggering coronal mass ejections, *Adv. Space Res.*, 2013, vol. 51, no. 11, pp. 1967−1980.

Schou, J., Scherrer, P.H., Bush, R.I., et al., Design and ground calibration of the Helioseismic And Magnetic Imager (HMI) instrument on the Solar Dynamics Observatory (SDO), *Sol. Phys.*, 2012, vol. 275, nos. 1−2, pp. 229−259.

Zagainova, Iu.S. and Fainshtein, V.G., How do fast impulse CMEs related to powerful flares but unrelated to eruptive filaments appear and move?, *Adv. Space Res.*, 2015, vol. 55, no. 3, pp. 822−834.

Zagainova, Iu.S., Fainshtein, V.G., Gromova, L.I., and Gromov, S.V., Stealth coronal mass ejections: Identification of source regions and geophysical effects, *Proceedings of Tenth Workshop "Solar Influences on the Magnetosphere, Ionosphere and Atmosphere,"* Primorsko, Bulgaria, 2018, pp. 13−18.

Translated by O. Pismenov